JOURNAL OF MATERIALS SCIENCE 26 (1991) 447–454

The fabrication of metal matrix composites by a pressureless infiltration technique

M. K. AGHAJANIAN, M. A. ROCAZELLA, J. T. BURKE, S. D. KECK
Lanxide Corporation, Newark, Delaware 19714-6077, USA

A novel technique for fabricating metal matrix composites by the spontaneous (pressureless) infiltration of filler preforms with molten aluminium alloys is described. Numerous reinforcing materials, including Al_2O_3 and SiC of various configurations, such as particles, agglomerates, and fibres, have been incorporated as fillers. The effects of processing variables, such as alloy chemistry, process temperature, and filler material, on the infiltration kinetics and resultant microstructures are discussed. Comparisons with existing infiltration technology and preliminary composite properties are presented.

1. Introduction

Metal matrix composites have been receiving significant attention in recent years, particularly in the area of processing techniques. In many instances the properties of a reinforced metal have been shown to provide a performance advantage over a monolithic metal, but the high cost of producing the composite has prohibited widespread commercial use. Of the many potential metal matrix systems, aluminium alloy matrix composites have been the object of much research, primarily due to the light weight, low cost, and ease of fabrication of aluminium [1]. Within the class of aluminium alloy matrix composites there exist two distinct material systems, namely (i) discontinuously reinforced composites, with the reinforcement taking the form of a particle, a platelet, a whisker, or a chopped fibre, and (ii) continuously reinforced composites, with the reinforcement being a unidirectional or a multidirectional array of continuous fibres.

Discontinuously reinforced aluminium alloys have been fabricated by various means, including solid-state processes, such as powder metallurgy techniques (blending of metal and ceramic powders followed by hot pressing) [2], and liquid-state processes, such as compocasting (blending ceramic powder and molten aluminium, agitating and casting) [3–5] and pressurized liquid-metal infiltration [6, 7]. The solid-state processes have been most successful to date, but are costly. Liquid-metal processes have the potential to be more economical; however, the non-wetting nature of many ceramics by molten aluminium, which results in poor ceramic/metal interfaces and incomplete infiltration, has been an obstacle [8]. For example, Girot *et al.* [5] found that a squeeze-casting process subsequent to compocasting was necessary to obtain a satisfactory composite with an Al–4.5Cu alloy matrix reinforced with chopped Al_2O_3 fibres.

Continuously reinforced composites have also been produced by both solid- and liquid-state methods. The primary solid-state process is diffusion bonding, where reinforcing fibres are sandwiched between sheets of aluminium alloy to form a tape. A composite is then formed through two hot-pressing operations, the first to consolidate the tape and the second to laminate several tapes together [9]. Liquid-phase processing of composites containing continuous reinforcement generally involves liquid–metal infiltration. The infiltration can either be pressure assisted, such as with squeeze casting [10, 11], or vacuum assisted [12].

The present paper discusses a novel liquid–metal infiltration technique for the production of aluminium alloy matrix composites containing either discontinuous or continuous reinforcement.* Via the use of proper process conditions, the infiltration occurs spontaneously (as used, spontaneously means without the aid of any externally applied pressure or vacuum). The requirements for infiltration, which include the use of a magnesium containing alloy and a nitrogenous atmosphere [13], and examples of mechanical and wear properties that can be achieved [14], have been previously presented. Herein, the bounds of the process are reviewed, the effects of the process conditions on infiltration rates and product microstructures are described, and examples of mechanical and thermal properties of the composites are reported. In addition, comparisons are made between the characteristics of the present infiltration process and the existing infiltration and wetting information available in the literature.

2. Experimental procedure

Two experimental arrangements were employed in this work, shown schematically in Fig. 1a and b. In both cases, an aluminium alloy ingot was placed above a loose bed of reinforcement material that was contained within a refractory vessel. The alloy/filler pairs were then placed into a controlled atmosphere

*Process technology patented by Lanxide Corporation and tradenamed the PRIMEX™ pressureless metal infiltration process.

0022–2461/91 $03.00 + .12

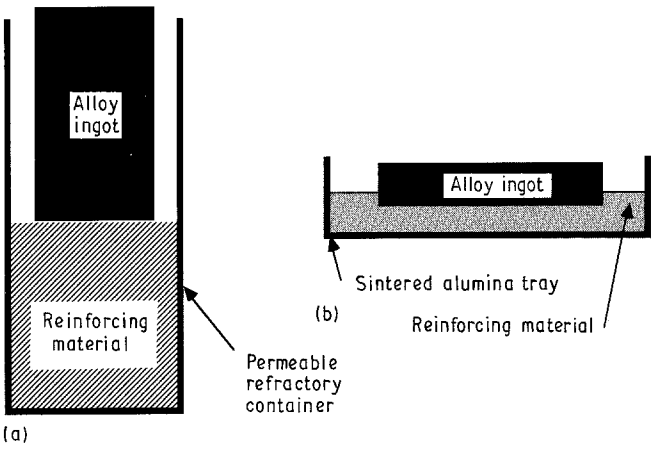

Figure 1 Schematic drawing of the experimental arrangements used to fabricate the metal matrix composites: (a): "Infinite" column of filler to determine infiltration kinetics, and (b) fixed quantities of alloy and filler to compare nitride formation.

furnace that was evacuated to 1×10^{-2} torr (1 torr = 133.322 Pa) at room temperature and back-filled with an atmosphere that was nitrogen-containing and nominally oxygen-free until a positive flow was obtained. To prevent unwanted gases from entering the furnace chamber, all experiments were conducted under a slight positive pressure that was achieved by bubbling the exit gas through a 25 mm column of oil. The furnace was ramped to temperature at a rate of 200 °C hr^{-1}, held at temperature for the specified time, and allowed to cool to 675 °C, at which time the samples were removed from the furnace and cooled to room temperature. All the ceramic fillers were obtained commercially. The particulate fillers were specified to be at or less than a specific sieve size, and are referred to by average particle size in the text.

The first experimental arrangement (Fig. 1a) employed a gas-permeable refractory vessel that had inside dimensions of about 65 mm diameter and 150 mm high. The aluminium alloy had a mass of about 500 g in each case, and the filler material had a height that was great enough to prevent full infiltration under the process conditions (i.e. a more-or-less infinite column of filler material). After processing, the amount of infiltration (distance from original alloy/filler interface) for the specific process conditions was measured, and the composite was sectioned and examined both macro- and microstructurally. The measurements of infiltration distance per process time include both the incubation period prior to the start of infiltration and the time during which infiltration occurs, and thus provide engineering kinetics rather than a true infiltration rate. As used herein, the terms kinetics and rate refer to this engineering value.

The second experimental arrangement (Fig. 1b) employed fixed quantities of alloy (about 50 mm × 25 mm × 12 mm) and filler (about 70 g), and contained them in a sintered alumina tray measuring about 100 mm × 45 mm × 20 mm. After infiltration, the per cent weight gain of the samples was calculated (change in weight of the sample divided by the original alloy weight). Because the infiltration occurs in a nitrogenous atmosphere, aluminium nitride precipitates may form within the aluminium alloy matrix. The per cent weight gain provides a measure of the amount of aluminium nitride that forms during processing. For comparison, the total conversion of pure aluminium to aluminium nitride produces a weight gain of 52%. Because this experimental arrangement produced a constant volume of composite in all cases where full infiltration occurred, the weight gains of many experiments could be directly compared, thus indicating the effect of the process conditions on the formation of aluminium nitride (ignoring any weight losses due to volatilization of high vapour pressure species).

Using an experimental arrangement similar to that shown in Fig. 1b, several plates measuring about 200 mm × 100 mm × 25 mm were fabricated and characterized. The processing conditions for the production of the plates were such that minimal AlN would form. Measurements of tensile strength were made using flat, hour-glass-shaped specimens machined from the plates. The specimens had outside dimensions of 150 mm × 12.5 mm × 2.5 mm with a 20 mm long reduced section having a width of 8.75 mm. The reduction in width to the reduced section was accomplished with a 75 mm radius. The specimens were tested at room temperature with a Sintech universal testing machine under displacement control at a cross-head speed of 1 mm min^{-1}. Additionally, each specimen was instrumented with a strain gauge which provided a measure of the strain to failure.

The elastic constants were measured at room temperature using the resonance (standing wave) technique [15]. The Young's modulus and shear modulus were determined from the flexural and torsional models of vibration, respectively, on rectangular bars. Poisson's ratio was then calculated as $(E/2G) - 1$. The values of Young's modulus obtained with the resonance technique were confirmed by the stress–strain data obtained during the tensile tests. The coefficient of thermal expansion was determined by measuring the displacement induced when strain–gauge instrumented samples were soaked at a range of temperatures from 25 to ~ 100 °C. The measurements compensated for the expansion of the gauge. The thermal conductivity was calculated as the product of the density, the thermal diffusivity, and the specific heat. The thermal diffusivity and specific heat were measured by laser pulse and calorimetric techniques, respectively.

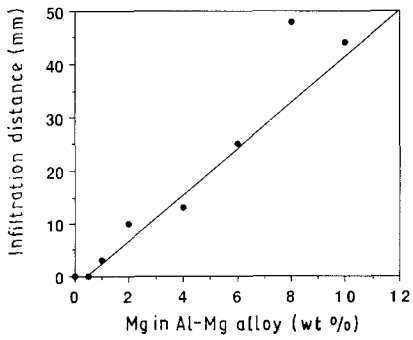

Figure 2 Relationship between magnesium content in an Al–Mg alloy and infiltration kinetics (obtained using process conditions of a 5 h soak at 900 °C, a nitrogen atmosphere, and an 18 μm fused Al_2O_3 filler).

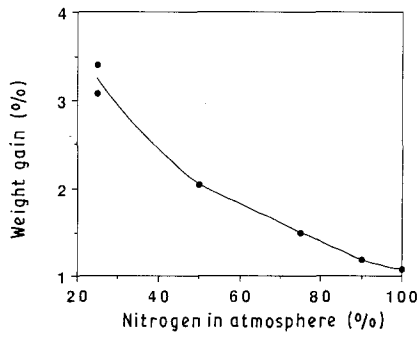

Figure 3 Dependence of unit weight gain (measure of AlN formation) on per cent nitrogen in an N_2/Ar atmosphere (obtained using alloy Al-10 Mg, a 66 μm fused Al_2O_3, and process conditions of a 4 h soak at 800 °C).

3. Results

3.1. Infiltration experiments

Initial experimentation [13] demonstrated that pressureless infiltration of molten aluminium alloys into compacts or loose beds of various reinforcing materials could occur if the correct process conditions were employed. The critical process conditions were found to be the alloy composition (specifically the magnesium content), the process temperature, the process time, and the nitrogen content of the atmosphere. It was observed that the use of a magnesium-containing aluminium alloy and a nitrogenous atmosphere in conjunction with an appropriate process temperature and dwell at temperature resulted in infiltration. No infiltration occurred without both magnesium in the alloy and a nitrogenous atmosphere. The following experiments were performed to provide kinetic data and to determine the bounds of the process.

The effect of the magnesium content in a binary Al–Mg alloy on the infiltration kinetics was determined using the experimental arrangement in Fig. 1a, with the result shown in Fig. 2. The reinforcing material in these experiments was an 18 μm fused Al_2O_3 grain that was simply poured into the refractory vessel. The process time and temperature were fixed at 5 h and 900 °C, respectively, and the atmosphere was nominally 100% N_2. The magnesium content was shown to be a significant variable, with increases in magnesium content resulting in an increased amount of infiltration. Although limited, the data suggest a linear relationship between magnesium content and amount of infiltration. Additionally, the data show that no infiltration occurs until a critical magnesium content is reached. The critical level changes with process conditions, but for the present case it is between 0.5 and 1 wt % Mg, with no infiltration occurring with alloy Al–0.5 Mg and 3 mm of infiltration occurring with alloy Al–1 Mg.

The effect of the nitrogen content of the atmosphere on the infiltration process was determined by conducting experiments in atmospheres ranging from 100% N_2 to 100% Ar. Using the experimental arrangement in Fig. 1b, alloy Al–10 Mg, a 66 μm fused Al_2O_3 grain, and process conditions of a 4 h soak at 800 °C, no infiltration occurred in 100% Ar, only partial infiltration occurred in 10% N_2/90% Ar and full infiltration occurred when the nitrogen content equalled or exceeded 25%.

In addition to affecting the amount of infiltration, the atmosphere affected the quantity of nitride that formed within the product. Fig. 3 plots the unit weight gain against the per cent nitrogen in the atmosphere for all of the samples where full infiltration occurred. At high percentages of nitrogen, where infiltration was rapid, little AlN formed, whereas in dilute atmospheres, where infiltration was slow, observable levels of AlN were evident. Fig. 4 shows the microstructures obtained in 100% N_2 and in 10% N_2/90% Ar. When present, AlN tended to form preferentially at the matrix/filler interface.

At a constant magnesium level and a fixed nitrogen content, various other process variables can affect the infiltration behaviour. Fig. 5 plots infiltration distance against temperature for otherwise constant process conditions, and shows that infiltration increased in an approximately linear manner with temperature. Additionally, the data show that there is a critical temperature required to induce spontaneous infiltration for a given set of process conditions. The present data show that no infiltration occurred at 750 °C using alloy Al–8 Mg, an 18 μm fused Al_2O_3 filler, a 5 h dwell at temperature, and a nitrogen atmosphere, whereas 19 mm infiltration occurred at 800 °C.

In addition to kinetics, the process temperature strongly affected the quantity of AlN that formed within the aluminium alloy matrix. Fig. 6 plots the unit weight gain against temperature for samples produced using the second experimental arrangement. The experiments employed alloy Al–10 Mg, a 66 μm fused Al_2O_3 grain and process conditions of a 4 h soak at temperature in nitrogen. The results demonstrate that as the process temperature increases, the quantity of AlN that forms also increases, and that the increase is approximately exponential over the temperature range investigated. These changes can be observed microstructurally, and appear similar to those evinced in Fig. 4.

As shown in Fig. 2, the magnesium content of the alloy has a marked effect on the infiltration kinetics. To a lesser extent, other alloying elements also affect the infiltration behaviour. For instance, silicon additions to the alloy were shown to enhance infiltration.

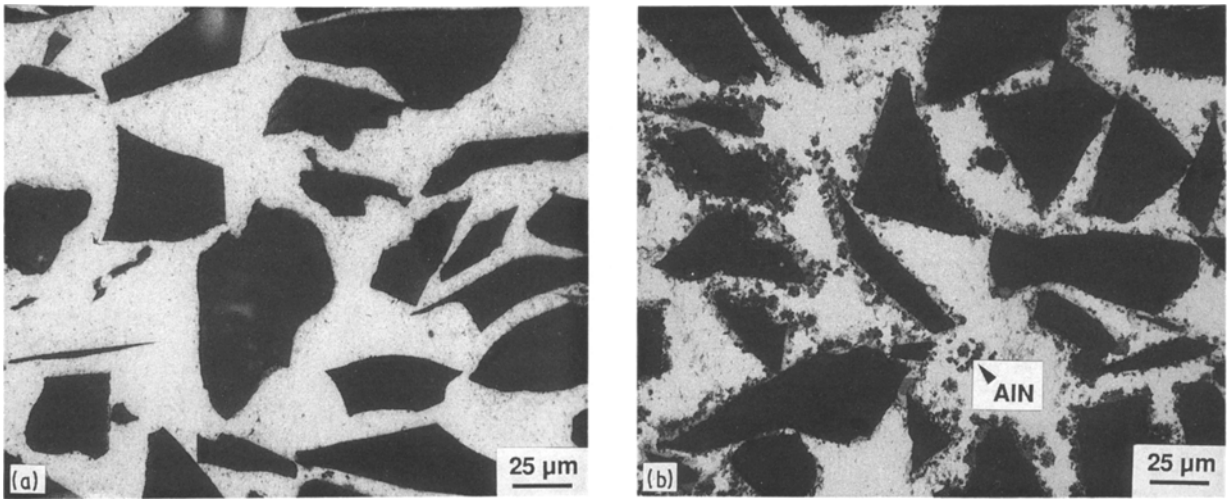

Figure 4 Effect of furnace atmosphere on product microstructure: (a) 100% N_2, and (b) 10% N_2/90% Ar.

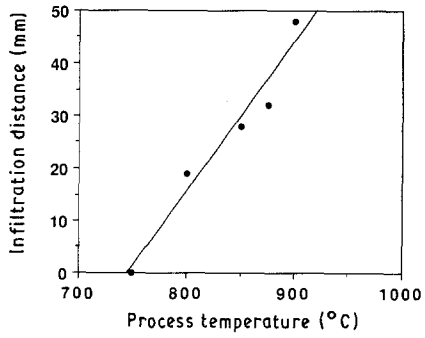

Figure 5 Variation of infiltration kinetics with process temperature (obtained using alloy Al–8 Mg and process conditions of a 5 h soak at temperature, a nitrogen atmosphere, and an 18 μm fused Al_2O_3 filler).

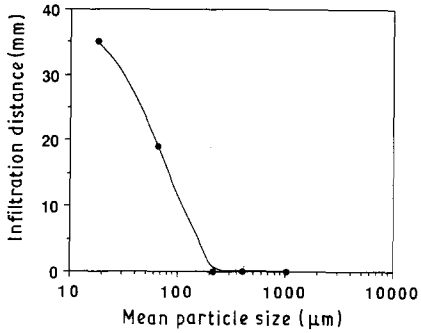

Figure 7 Relationship between fused Al_2O_3 particle size and infiltration rate (obtained using alloy Al–10 Mg and a 15 h soak at 800 °C).

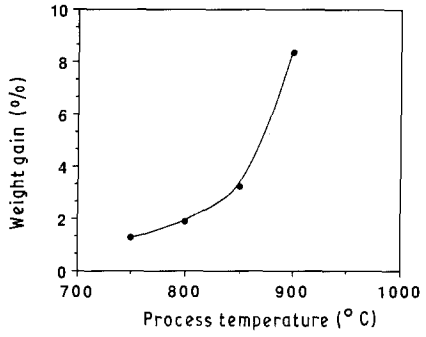

Figure 6 Relationship between process temperature and AlN formation (unit weight gain) in aluminium alloy matrix (obtained using alloy Al–10 Mg, a 66 μm fused Al_2O_3 filler, and process conditions of a 4 h dwell at temperature in nitrogen).

Using the experimental arrangement in Fig. 1a, a 5 h dwell at 900 °C in nitrogen, and an 18 μm fused Al_2O_3 filler, infiltration distances of 25 and 44 mm were obtained with alloys Al–6 Mg and Al–6 Mg–8 Si, respectively. Unlike silicon, copper additions retarded the process kinetics. A 10 h dwell at 800 °C in nitrogen yielded 35 mm infiltration into an 18 μm fused Al_2O_3 filler with alloy Al–10 Mg, whereas only 12 mm infiltration occurred under the same process conditions with alloy Al–10 Mg–3Cu.

Fig. 7 plots infiltration distance against filler particle size using fused Al_2O_3 particles with average particle sizes of about 18, 66, 216, 406, and 1035 μm. The data show that the rate of infiltration into the finer particle sizes was far greater than that into the coarse particles. Using the experimental arrangement in Fig. 1a, alloy Al–10 Mg, a dwell at 850 °C of 5 h, and a nitrogen atmosphere, infiltration was obtained into the 18 and 66 μm particles but no infiltration occurred into the 216 μm and larger particles.

The pressureless infiltration technique is applicable to the production of composites containing a wide range of reinforcement types. Examples of Al_2O_3 particle-reinforced composites are shown in Fig. 4. Fig. 8 provides examples of Al_2O_3 platelet and continuous fibre-reinforced aluminium alloy matrices. Owing to the marked effect of filler size on the infiltration process it was not possible to isolate the effect of filler geometry and in turn quantitatively determine its effect on infiltration rate; however, it was found that filler geometry did not significantly affect the infiltration process. Similarly, the pressureless infiltration technique is applicable to many filler materials. In addition to SiC and Al_2O_3, reinforcement materials that have been utilized include TiB_2, MgO, graphite coated (by chemical vapour deposition) with SiC, and AlN. Microstructures of composites containing 66 μm SiC and 10 μm TiB_2 are shown in Fig. 9.

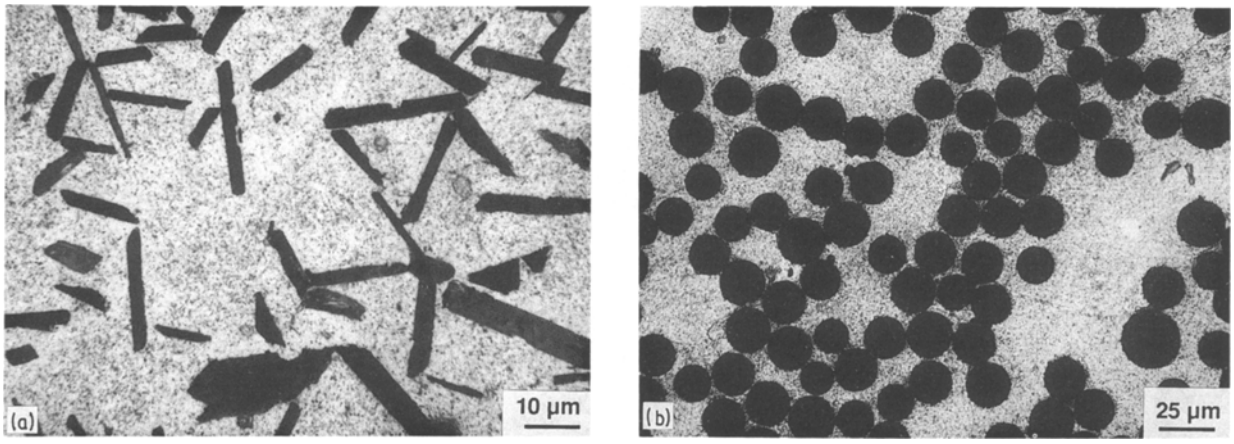

Figure 8 Examples of Al_2O_3-reinforced aluminium alloy matrix composites: (a) platelets and (b) continuous fibres.

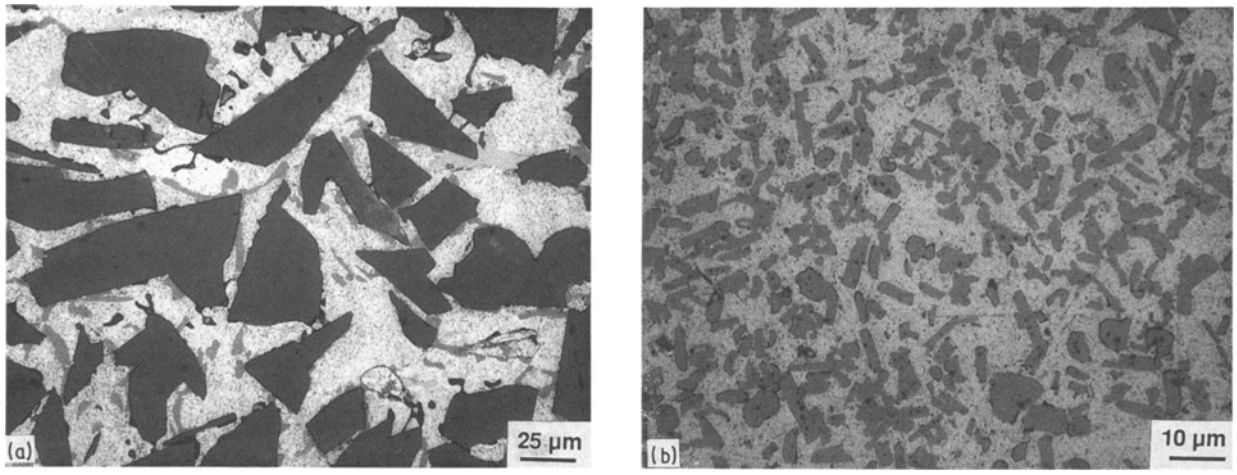

Figure 9 Examples of particle-reinforced aluminium alloy matrix composites: (a) SiC and (b) TiB_2.

3.2. Property data

Mechanical property measurements were made on three tabular Al_2O_3 particle-reinforced composites in both the as-fabricated (F) and solution-treated and naturally aged (T4) conditions, with the results shown in Table I. The solution treatment was accomplished by an 18 h soak at 435 °C followed by a quench into 80 °C water. The three composites were produced with the same alloy (Al–10 Mg), but with different particle sizes of Al_2O_3 (− 250, − 149, and − 44 μm). An attempt was made to keep the respective volume fractions of alloy and filler constant, but due to difficulty associated with the compaction of fine powders, the − 44 μm Al_2O_3 reinforced sample had a somewhat lower volume fraction of particles. The volume fractions of Al_2O_3 in the composites that were tested were 56%, 57%, and 51%, from coarse to fine.

The results show that the ultimate tensile strength and the strain to failure were inversely related to the size of the reinforcement, and that the elastic properties were related to the volume fraction of filler. The elastic properties were not affected by reinforcement size at constant volume fraction, but the decrease in Al_2O_3 content from the samples with the coarse fillers (− 250 and − 149 μm) to the sample with the fine filler (− 44 μm) resulted in lower values of the Young's and shear moduli, and a higher value for Poisson's ratio.

Thermal property measurements were made on two SiC reinforced composites. Both composites were in the as-fabricated condition. Again, the composites were produced with the same alloy (an Al–Mg alloy with 15 wt % Si added to minimize Al–SiC reactions), but with different particle sizes of SiC (about 216 and 66 μm). Both composites had about the same loading of SiC, with respective volume fractions of 54 and 51, for the coarse and the fine filler. The data, shown in Table II, demonstrate that both the coefficient of thermal expansion and the thermal conductivity are not a function of reinforcement size at nearly constant volume fraction of reinforcement. Additionally, both composites exhibited a drop in thermal conductivity from room temperature to 200 °C.

4. Discussion

4.1. Wetting and infiltration

The pressureless infiltration of molten aluminium alloys into preforms or loose beds of reinforcing materials has not been previously observed except in various specialized cases, such as when the filler is reactive (e.g. Al–B_4C composites [16]). Edwards and

TABLE I Mechanical properties of Al_2O_3-reinforced composites fabricated with alloy Al–10 Mg

Reinforcement	Condition	Ultimate tensile strength (MPa)	Strain to failure (%)	Young's modulus (GPa)	Shear modulus (GPa)	Poisson's ratio
– 250 μm Al_2O_3	F	242	0.169	180	72	0.26
– 149 μm Al_2O_3	F	285	0.201	180	71	0.27
– 44 μm Al_2O_3	F	457	0.476	165	65	0.34
– 250 μm Al_2O_3	T4	286	0.185			
– 149 μm Al_2O_3	T4	318	0.236			
– 44 μm Al_2O_3	T4	506	0.563			
None [22]	T4	331	16	65		

TABLE II Thermal properties of SiC-reinforced composites

Reinforcement	Coefficient of thermal expansion 25 to 100 °C ($1 \times 10^{-6} K^{-1}$)	Thermal conductivity ($W m^{-1} K^{-1}$)		
		25 °C	100 °C	200 °C
216 μm SiC	9.2	166	139	128
66 μm SiC	9.4	171	140	133
None [22]	22.0	155		

Olsen [7] found that aluminium would not spontaneously infiltrate SiC, even under process conditions where the contact angle for the Al/SiC system was less than 90°. They suggested that factors such as interfacial reaction kinetics or fluid flow end effects could have inhibited infiltration, claiming that with a contact angle less than 90°, spontaneous infiltration would have occurred if the surface tension force was the only resistance to infiltration.

The enhanced wetting of ceramic materials resulting from the addition of magnesium to an aluminium alloy is well documented [3, 4, 6, 17, 18]. Several mechanisms are generally discussed when the role of magnesium is considered. Banerji *et al.* [19] claim that the addition of an alloying element can enhance the wetting of a solid surface in three ways, namely (i) by reducing the surface tension of the alloy, (ii) by decreasing the solid–liquid interfacial energy, and (iii) by promoting a chemical reaction at the solid–liquid interface. McCoy *et al.* [3] state that magnesium is effective in reducing the surface tension of the melt and inducing interfacial reactions. Oh *et al.* [6], who found magnesium to significantly improve wettability, believe that the promotion of interfacial reactions is the most active mechanism for enhancing the wetting of a solid ceramic surface with a molten aluminium alloy.

Few relationships exist that examine the role of these variables. The Washburn equation, which is often used to measure pore-size distributions by the mercury porosimetry technique [20], provides the pressure, P, required to infiltrate a pore of given radius. It can be expressed as

$$P = (2\gamma_{LV}\cos\theta)/r \quad (1)$$

where γ_{LV} is the liquid–vapour surface energy (surface tension), θ is the liquid–solid contact angle, and r is the pore or capillary radius. Thus, by changing both the surface tension of the molten alloy and the liquid–solid contact angle (through interfacial reactions), magnesium additions to an aluminium alloy can affect the pressure required for infiltration.

Little information is available in the literature on the effect of a nitrogen atmosphere on wetting. McCoy *et al.* [3] found that when fabricating aluminium alloy matrix composites via compocasting, the use of a nitrogen atmosphere and a bubble-degassing step with nitrogen yielded composites with much lower porosity than those produced similarly with argon, but these results may not be associated with enhanced wetting.

The results of the present work demonstrate that the combination of magnesium in the alloy and a nitrogenous atmosphere leads to the spontaneous infiltration of aluminium alloys into ceramic fillers. Although a complete explanation is beyond the scope of this paper, some comparisons can be drawn to literature observations of wetting of non-metals by molten aluminium. As previously stated, magnesium decreases the surface tension of a molten aluminium alloy. This alone does not induce spontaneous infiltration, but a nitrogen atmosphere may cause a further reduction in the surface tension, thus promoting wetting. Additionally, the reactivity of magnesium induces interfacial reactions with solid ceramic surfaces. These reactions typically are not enough to promote spontaneous wetting, but in combination with a nitrogen atmosphere they may change or be altered, thus allowing the observed infiltration.

For a given set of process conditions there is a threshold or critical magnesium content required to promote spontaneous infiltration, as is shown in Fig. 2. McCoy *et al.* [3] found a similar effect when producing TiB_2 platelet-reinforced aluminium alloy composites by compocasting. Without enough magnesium in the alloy, the TiB_2 platelets were rejected, whereas at magnesium levels greater than the threshold value, the TiB_2 platelets were readily wetted. While working at temperatures near the liquidus, they found the threshold magnesium level to be between 2 and 3 wt %.

The effect of the viscosity of the molten aluminium alloy on infiltration is demonstrated by the results obtained with the silicon- and copper-containing Al–Mg alloys. Because they are relatively nonreactive, it is unlikely that either silicon or copper contribute to interfacial reactions. However, they both cause significant changes to the viscosity of molten aluminium.

For instance, the viscosities at 900 °C of pure aluminium Al–5Si, and Al–5Cu are 0.91, 0.85, and 1.01 cP (1cP = 10^{-3} N m^{-2}), respectively [21]. The addition of silicon to the alloy resulted in an increased rate of infiltration, whereas the addition of copper produced the opposite effect. This result follows various models proposed in the literature. For instance, Martins *et al.* [8] have developed an intrinsic infiltration rate parameter, ϕ, which can be expressed as

$$\phi = (r\gamma_{LV}\cos\theta)/2\mu \quad (2)$$

where $(r\gamma_{LV}\cos\theta)$ is the surface tension force term and μ is the viscosity of the melt. ϕ can be used as a figure of merit where high values infer favourable infiltration kinetics. Thus, increased infiltration rates are predicted for alloys with lower viscosities.

It is well documented that filler particle size has a marked effect on infiltration. McCoy *et al.* [3] suggest that as the filler particle size decreases, an increased energy (pressure) is required for wetting to occur because the metal must deform to a smaller radius, thereby making infiltration difficult. This is supported by Equations 1 and 2, where increases in the capillary radii (as the particle size increases, the capillaries between the particles also increase) result in a decrease in the pressure required for infiltration to occur and an increase in the infiltration rate parameter, respectively. The results of the present work (Fig. 7) contradict those in the literature. It was found that the fine fused Al_2O_3 particles were easily wet, and as the particle size increased, the tendency for infiltration was reduced. This difference in behaviour is attributed to the nature of the various processes. In the present process, where wetting is preferred (i.e. the infiltration occurs spontaneously), the dominant variable with respect to particle size is surface area. Smaller particles provide a greater area of wettable surface, thus enhancing infiltration. In other processes wetting is not preferred and infiltration is achieved via the use of external pressure or agitation. The resistance to infiltration is then dominated by the force required to move metal into the channels (capillaries) between the particles. In this case, large particles are preferred.

4.2. Mechanical and thermal properties

Owing to the favourable wetting obtained with this process, there is a strong potential for the production of pore-free composites with high structural integrity. Delannay *et al.* [1] state that enhanced wetting typically results in increased strength at the metal–ceramic interface, thus enhancing the mechanical properties of the composite. Burke *et al.* [14] presented the mechanical properties of Al_2O_3 and SiC particle-reinforced aluminium alloy composites in the as-fabricated condition that were produced by the present process. They found that, as suggested, the properties of the Al_2O_3 reinforced composites can be quite favourable, exceeding the strength of the base alloy in some cases. The strength of the SiC reinforced composites, however, was found to be only about 75% of that of the Al_2O_3-reinforced composites at constant volume fraction and size of filler. The lower strength was attributed to the high silicon content of the alloys used in conjunction with the SiC filler.

The tensile strengths of the Al_2O_3 reinforced composites produced in the present work with alloy Al–10 Mg (Table I) can also be greater than the strength of the base alloy, depending on the size of the Al_2O_3 filler. Aluminium alloy 520.0 (nominally Al–10 Mg) has an ultimate tensile strength of 331 MPa in the T4 condition [22], whereas the strengths in the T4 condition of the composites containing the -250, -149, and -44 μm Al_2O_3 were 286, 318, and 506 MPa, respectively (Table I). Examination of the fracture surfaces revealed that, as desired, the mode of fracture was predominantly transgranular (i.e. the fracture occurred through, rather than around, the Al_2O_3 particles).

McDanels [23] found that the strengths of discontinuously reinforced SiC/Al alloy composites were controlled by the strengths of the matrix alloys when all other parameters were constant, and thus was able to produce stronger composites via the use of heat-treatments. The same result was obtained in the present study with samples in the T4 condition exhibiting greater strengths than otherwise identical samples in the as-fabricated condition (Table I). However, the increases in strength were only moderate, with gains of 18%, 12%, and 11%, respectively, for the -250, -149, and -44 μm fillers. This may be due to the use of a heat-treatment schedule that was developed for the base alloy. Reviewing the work of others, Lewandowski [24] found that the heat-treatment schedules for monolithic alloys are generally not optimum for composites.

The SiC-reinforced composites do not presently possess the structural properties of the Al_2O_3-reinforced composites, but the combination of the favourable thermal properties of SiC and the ability of the pressureless infiltration process to accommodate high filler loadings allows the formation of composites with very favourable thermal characteristics. Specifically, SiC has a high thermal conductivity (126 W m^{-1} K^{-1} [25] compared to 29 W m^{-1} K^{-1} for Al_2O_3 [26]) and a low coefficient of thermal expansion (4.0×10^{-6} K^{-1} [25] compared to 8.1×10^{-6} K^{-1} for Al_2O_3 [26]). This allows the fabrication of aluminium alloy matrix composites that maintain the high thermal conductivity of the base metal while possessing coefficients of thermal expansion that match or nearly match lower expansion materials, such as steels, various ceramics, and semiconductors. The data in Table II demonstrate that a significant reduction in the coefficient of thermal expansion from the base alloy can be achieved by infiltrating a loose bed of SiC particles. Further reductions in the coefficient of thermal expansion can be realized by infiltrating more highly loaded SiC fillers.

5. Conclusions

A novel process for the production of metal matrix composites containing either continuous or discontinuous reinforcement is reported. It involves the

spontaneous (i.e. without the aid of any externally applied pressure or vacuum) infiltration of aluminium alloys into loose beds or compacts of reinforcing materials by proper control of the process conditions. The processing data presented show that there are two requirements for the wetting to occur, namely (i) that the aluminium alloy contains magnesium and (ii) that the atmosphere be nitrogenous. The infiltration kinetics were shown to be strongly affected by the process variables. Increases in temperature and magnesium content resulted in increased infiltration rates. AlN precipitates can form within the aluminium alloy matrix, particularly at high temperatures and in low nitrogen-content atmospheres. Additions of silicon to the alloy enhanced infiltration, whereas copper additions retarded infiltration. With a fused Al_2O_3 filler, infiltration slowed as particle size increased.

Owing to the enhanced wetting provided by this process, and thus the good metal–ceramic bond that is achieved, the Al_2O_3 particle-reinforced aluminium alloy matrix composites show favourable structural properties. The SiC particle-reinforced composites possess a useful combination of high stiffness, high thermal conductivity, and low coefficient of thermal expansion, in most part due to the high particle loading obtained in the present samples.

Acknowledgements

The authors thank R. J. Wiener and W. R. Steininger, Lanxide Corporation, for technical assistance.

References

1. F. DELANNAY, L. FROYEN and A. DERUYTTERE, *J. Mater. Sci.* **22** (1987) 1.
2. I. J. TOTH, W. D. BRENTNALL and G. D. MENKE, *J. Metals* **24** (1972) 19.
3. J. W. McCOY, C. JONES and F. E. WARNER, *SAMPE Q.* **19**(2) (1988) 37.
4. S. DAS, T. K. DAN, S. V. PRASAD and P. K. ROHATGI, *J. Mater. Sci. Lett.* **5** (1986) 562.
5. F. A. GIROT, P. KARANDIKAR, A. P. MAJIDI and T. W. CHOU, *Proc. Int. SAMPE Symp.* **33** (1988) 1260.
6. S.-Y. OH, J. A. CORNIE and K. C. RUSSELL, *Ceram. Engng Sci. Proc.* **8** (7–8) (1987) 912.
7. G. R. EDWARDS and D. L. OLSEN, Annual Report Under ONR Contract No. N00014-85-K-0451, July 1987.
8. G. P. MARTINS, D. L. OLSEN and G. R. EDWARDS, *Met. Trans.* **19B** (1988) 95.
9. D. J. LLOYD, *J. Mater. Sci.* **19** (1984) 2488.
10. T. W. CLYNE and J. F. MASON, *Met. Trans.* **18A** (1987) 1519.
11. S. K. VERMA and J. L. DORCIC, *Ceram. Engng Sci. Proc.* **9**(7–8) (1988) 579.
12. F. FOLGAR, *ibid.* **9** (7–8) (1988) 561.
13. M. K. AGHAJANIAN, J. T. BURKE, D. R. WHITE and A. S. NAGELBERG, *Proc. Int. SAMPE Symp.* **34** (1989) 817.
14. J. T. BURKE, M. K. AGHAJANIAN and M. A. ROCAZELLA, *ibid.* **34** (1989) 2440.
15. S. SPINNER and W. E. TEFFT, *ASME Proc.* **61** (1961) 1221.
16. A. J. PYZIK and I. A. AKSAY, US Pat. 4 702 770, October 1987.
17. J. A. CORNIE, A. MORTENSEN and M. C. FLEMINGS, in Proceedings of the Sixth International Conference on Composite Materials and the Second European Conference on Composite Materials (ICCM and ECCM), London, UK, Vol. 2, edited by F. L. Matthews, N. C. R. Buskell, J. M. Hodgkinson and J. Morton (Elsevier Applied Science, London, (1987) p. 2.297.
18. T. CHOH, R. KAMMEL and T. OKI, *Z. Metallkde* **78** (1987) 286.
19. A. BANERJI, P. K. ROHATGI and W. REIF, *Metallwiss. Technik* **38** (1984) 656.
20. A. LANE, N. SHAH and W. C. CONNER Jr, *J. Colloid Interface Sci.* **109** (1986) 235.
21. F. LIHL, E. NACHTIGALL and A. SCHWAIGER, *Z. Metallkde* **59** (1968) 213.
22. "Metals Handbook", Desk Edition, edited by H. E. Boyer and T. L. Gall (American Society for Metals, Metals Park, Ohio, 1985) pp. 6.48–6.62.
23. D. L. McDANELS, *Met. Trans* **16A** (1985) 1105.
24. J. J. LEWANDOWSKI, *SAMPE Q.* **20** (1989) 33.
25. C. H. McMURTY, W. D. G. BOECKER, S. G. SESHADRI, I. S. ZANGHI and J. E. GARNIER, *Amer. Ceram. Soc. Bull.* **56** (1987) 325.
26. R. KAMO and W. BRYZIK, *Ceram. Engng Sci. Proc.* **5**(5–6) (1984) 312.

Received 14 August 1989
and accepted 19 February 1990